JOURNAL OF MATERIALS SCIENCE **40** (2005) 145–154

Influence of the microstructure on the toughness of a duplex stainless steel UNS S31803

S. S. M. TAVARES, V. F. TERRA, J. M. PARDAL, M. P. CINDRA FONSECA
Departamento de Engenharia Mecânica, PGMEC, UFF, Rua Passo da Pátria, 156, CEP 24210-240, Niterói
E-mail: ssmtavares@ig.com.br

The microstructure of a duplex stainless steel UNS S31803 was varied by high temperature treatments (1300°C) followed by different cooling rates. A wide range of microstructures, with differents morphologies and phase proportions, were obtained by this way. Some samples were solution treated at 1000°C and fast cooled after the high temperature treatment. The impact toughness in all conditions were evaluated by reduced size (2.5 mm) Charpy impact tests. The highest toughness was obtained in the samples cooled in furnace from 1300 to 1000°C and then air cooled to room temperature. The microstructure at this condition was very fine with 55.4% of austenite. The lower toughness value was obtained in the water cooled sample, which presented only 17.1% of austenite and large grains of ferrite. The toughness of these and other microstructures was improved by the solution treatment.

1. Introduction

The use of duplex stainless steels (DSS) as structural and corrosion resistant materials is increasing markedly in recent years. The fine austenite-ferrite microstructure of these materials promotes an excellent combination of toughness and mechanical resistance, desirable for many applications in the chemical and petrochemical industries. The optimization of mechanical and corrosion resistance properties of wrought DSS is believed to be obtained for a phase proportion of 1:1 [1].

During welding operations the DSS is heated at high temperatures in the heat affected zone (HAZ). At the overheated region, where temperatures higher than 1300°C are reached, the steel becomes ferritic and the austenite phase appear during the cooling to room temperature. The problem of welding DSS is that fast cooling rates in the HAZ promote much less austenite than the desired amount (∼50%) and this may cause loss of toughness and corrosion resistance [2, 3]. This problem can be avoided by lowering the cooling rate with the proper control of heat imput, pre-heating and interpass temperatures. On the other hand, cooling rates must be high enough to avoid sigma phase, chromium carbide and α' precipitations in the 350–1000°C range [4].

In this work the microstructure of a UNS S31803 was varied by different high temperature treatments, simulating some situations found in the overheated zone of HAZ in DSS welds. The microstructures were also modified by a solution treatment at 1000°C after the high temperature treatments, simulating the effect of a post weld heat treatment.

2. Experimental

The DSS UNS S31803 analysed (composition shown in Table I) was received as plates of 4 mm in thickness. In the as received condition the DSS presented a fine microstructure with 55% of austenite (45% of ferrite) and the mechanical properties shown in Table I. The material was cut into samples of 58 × 13 × 4 (mm) and heat treated at 1300°C for 30 min. Four cooling conditions were employed: W—water cooling to room temperature (RT); O—oil cooling to RT; A—air cooling to RT; FA—cooling into furnace till 1000°C followed by air cooling to RT; and F—cooling into furnace to RT.

After the high temperature treatment, some samples were solution treated at 1000°C and water cooled. Table II presents all heat treatment conditions produced in this work.

The Charpy-V reduced size specimens (2.5 mm) were machined accordingly to the ASTM E23 standard [5]. The Charpy tests were realized at room temperature, using an universal impact test machine with maximum capacity of 300 J and precision of ±1 J. Two samples from each condition were tested, and when a discrepancy higher them 5% was observed a third sample was tested. Vickers hardness and microhardness were performed with 30 kgf and 50 g, respectively.

Metalographic samples were prepared and etched with Murakami's reagent for phase quantification or with 10% oxalic acid solution (electrolytic) to reveal grain boundaries. The austenite volume fractions were measured by quantitative metallography. Fracture analysis was conducted in a ZEISS scanning electron microscope. X-ray diffraction was carried out in a PHILLIPS® X-PERT diffractometer using Cu K_α radiation.

TABLE I Chemical composition of the DSS analysed steel

Chemical analysis (wt%)					Mechanical properties			
Cr	Ni	Mo	C	N	HV	E_{Charpy} (J)[a]	$\sigma_{L.E.}$ (MPa)	$\sigma_{L.R.}$ (MPa)
22.3	5.44	2.44	0.02	0.160	264	35.5 ± 1	503	805

[a]Reduced size specimens (2.5 mm).

TABLE II Heat treatments and samples identification

Identification	Heat treatment
W1	1300°C, water cooling to room temperature (RT)
W2	same as W1 plus solution treatment (1000°C/1 h, water cooling)
O1	1300°C oil cooling to RT
O2	same as O1 plus solution treatment (1000°C/1 h, water cooling)
A1	1300°C air cooling to RT
A2	same as A1 plus solution treatment (1000°C/1 h, water cooling)
FA1	1300°C furnace cooling to 1000°C, air cooling to RT
FA2	same as FA1 plus solution treatment (1000°C/1 h, water cooling)
F1	1300°C furnace cooling to RT
F2	same as F1 plus solution treatment (1000°C/1 h, water cooling)

3. Results

Fig. 1a–e show the microstructures obtained by the high temperature treatments with different cooling rates. The water cooled (W1) and the oil cooled (O1) samples presented equiaxial grains of austenite among with alotriomorphic austenite precipitated at the grain boundaries. This is also observed in the air cooled sample (A1), but with higher austenite content and some Widmanstätten morphology (Fig. 3). The samples FA1 and F1 presented the austenite phase with the equiaxial morphology (Fig. 1d and e).

Table III shows the austenite percentage obtained in each condition. Fig. 2 show that the solution treatment at 1000°C makes the amount of austenite to increase in the water cooled, oil cooled and air cooled samples. A small increase of $\%\gamma$ was also obtained from the condition FA1 (55.4%) to FA2 (59.8%). Fig. 3 presents the microstructure of the sample W2 showing that the austenite has precipitated as fine islands in the ferrite domains.

TABLE III Amount of austenite in each sample

Sample	$\%\gamma$	Sample	$\%\gamma$
W1	17.1 ± 4.1	W2	59.8 ± 3.6
O1	27.6 ± 3.7	O2	58.6 ± 4.2
A1	39.7 ± 9.6	A2	58.0 ± 11.0
FA1	55.4 ± 5.0	FA2	59.8 ± 12
F1	60.5 ± 12	F2	56.3 ± 7.8

Fig. 4 shows the energy absorbed values obtained in each condition. The sample FA1 presented the highest value of toughness after the high temperature treatment (36 J). This is certainly due to the higher austenite content and the effect of grain refinement caused by the austenite precipitation during the cooling. To illustrate this grain refinement Figs 5, 6 and 7 show the microstructures of samples W1, O1 and FA1 revealed by electrolytic etching in 10% acid oxalic solution. The fast cooled samples (W1 and O1) present coarse grains of ferrite, while the FA1 sample present a very fine microstructure. Although the corrosion resistance will be subject of another article, it is worth noting the preferential attack of the ferrite phase in the fast cooled samples. This is attributed to precipitates of Cr_2N in the ferrite (see Fig. 8). These particles also contribute to the poor toughness and higher hardness of the fast cooled samples [1, 3].

Figs 9 and 10 show the hardness and microhardness values before and after the solution treatment. The microhardness of the ferrite phase after the solution treatment in samples W2, O2 and A2 could not be measured since there were many austenite particles dispersed into the ferrite matrix (Fig. 3). From Fig. 9 the minimum

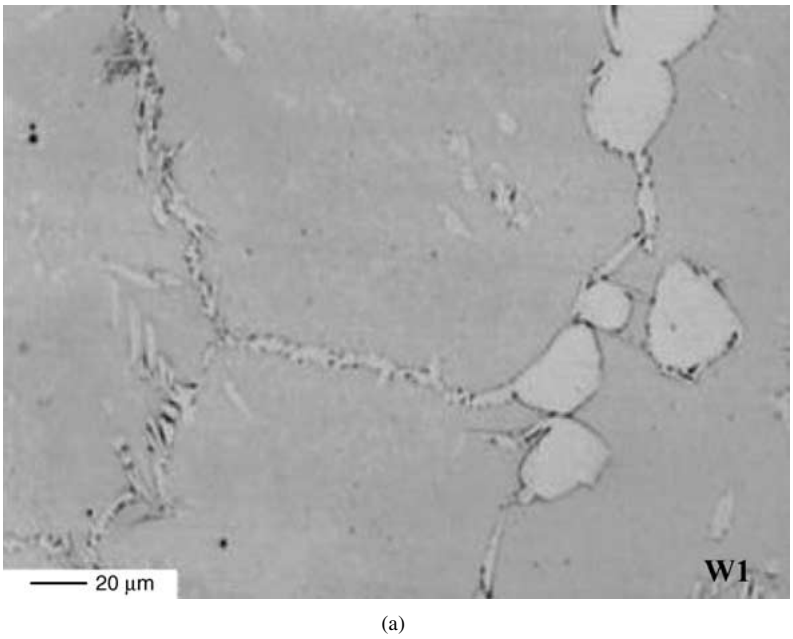

(a)

Figure 1 Microstructure of samples: (a) W1, (b) O1, (c) A1, (d) FA1, and (e) F1. (*Continued*)

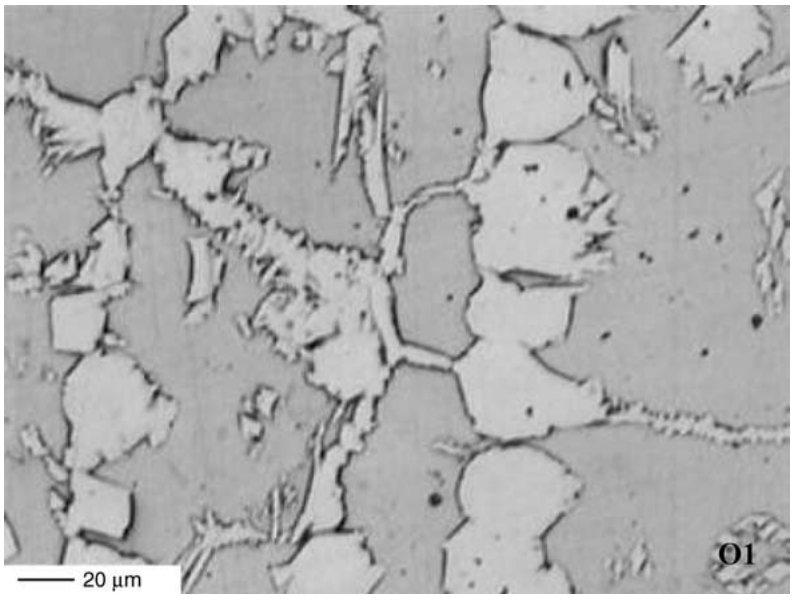

(b)

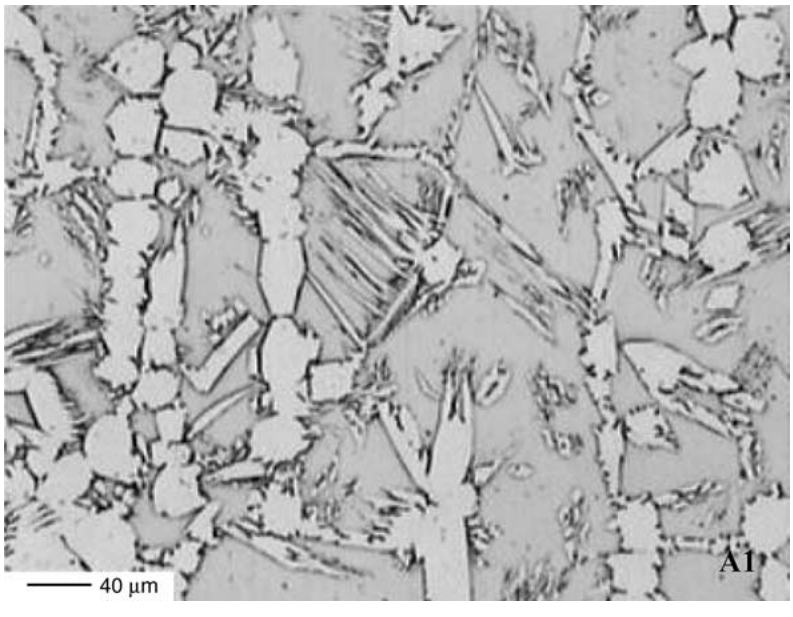

(c)

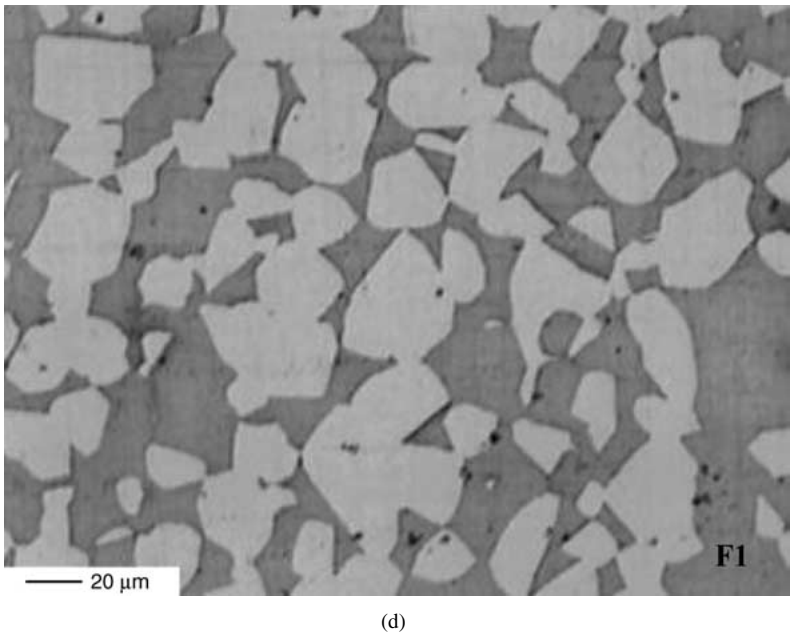

(d)

Figure 1 (*Continued*)

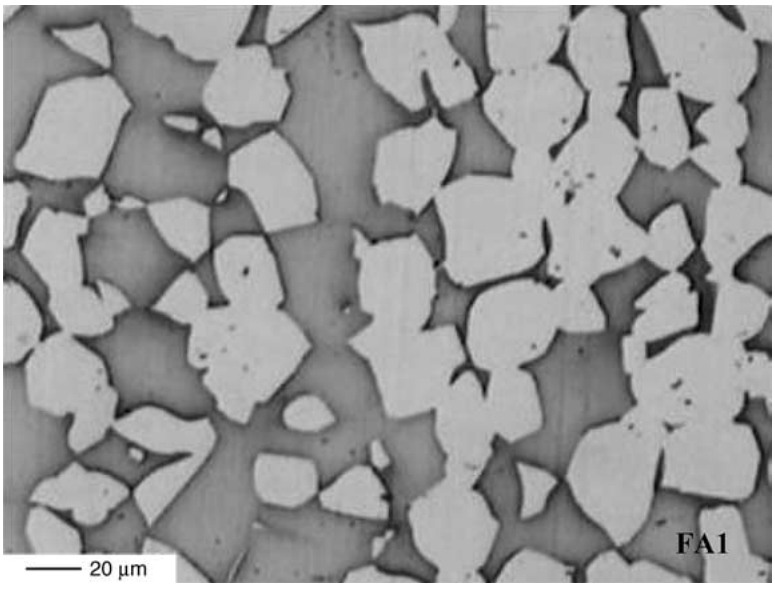

(e)

Figure 1 (*Continued*)

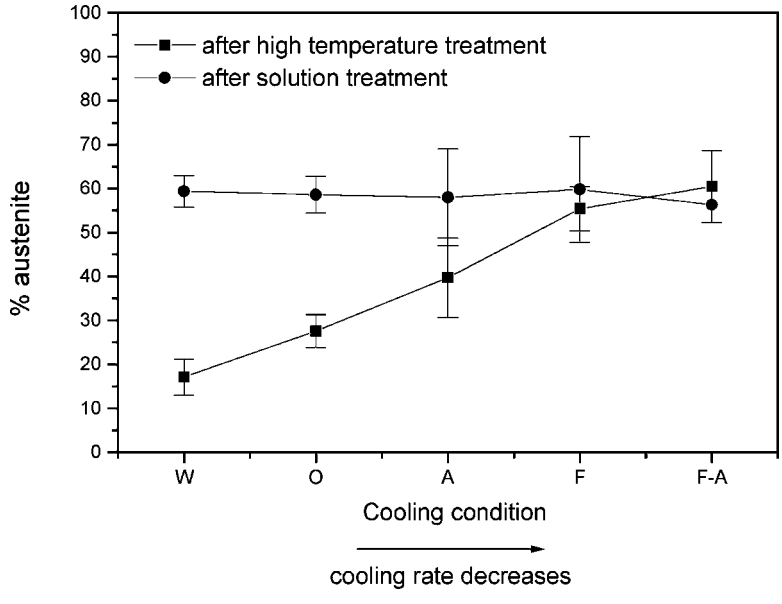

Figure 2 Austenite content as function of cooling condition before and after the solution treatment.

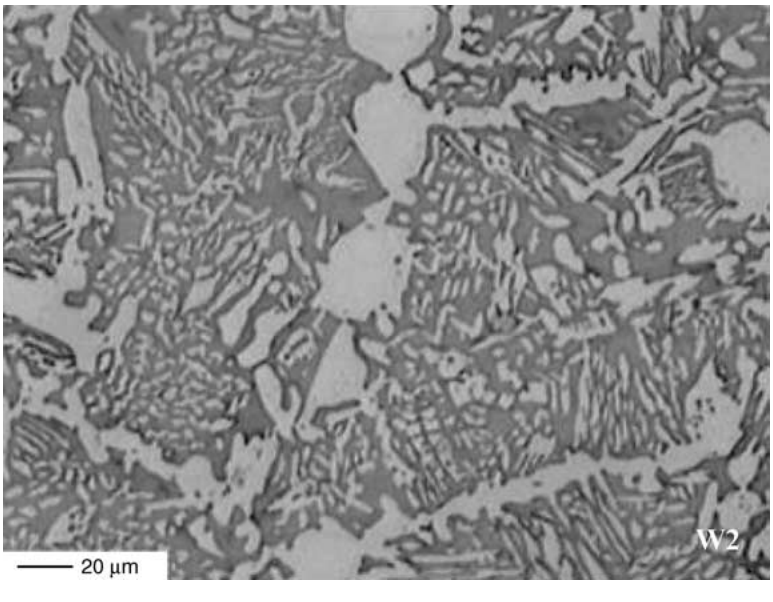

Figure 3 Microstructure of the water cooled and solution treated sample (W2).

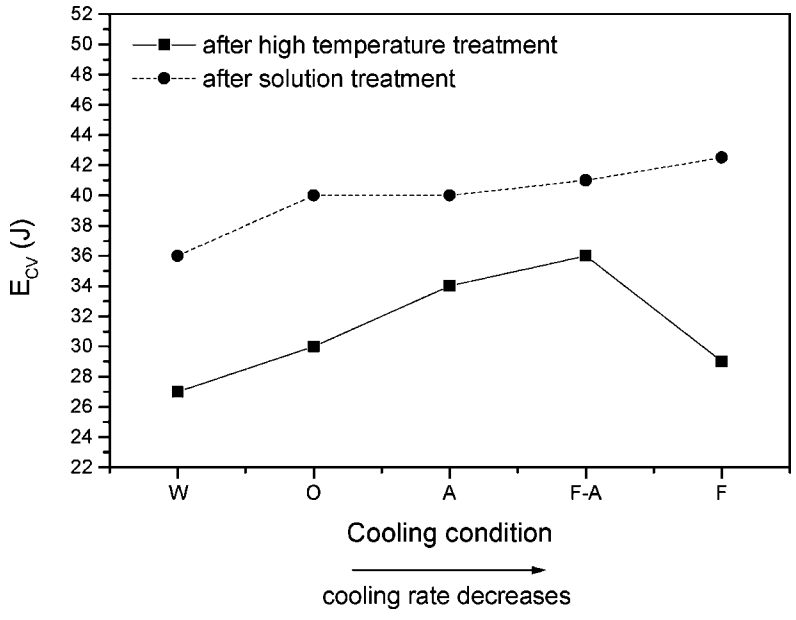

Figure 4 Impact absorved energy as function of cooling condition before and after the solution treatment.

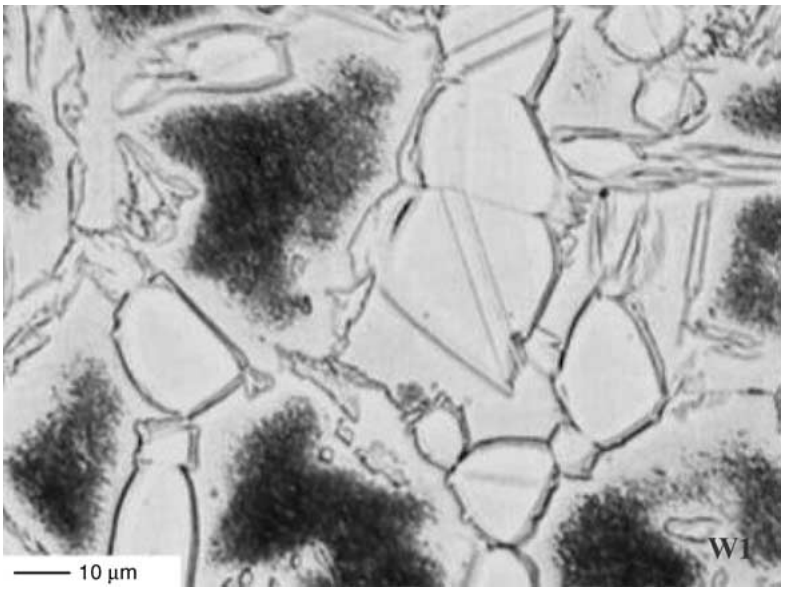

Figure 5 Microstructure of the water cooled sample (W1) revealed by electrolytic etch in oxalic acid solution.

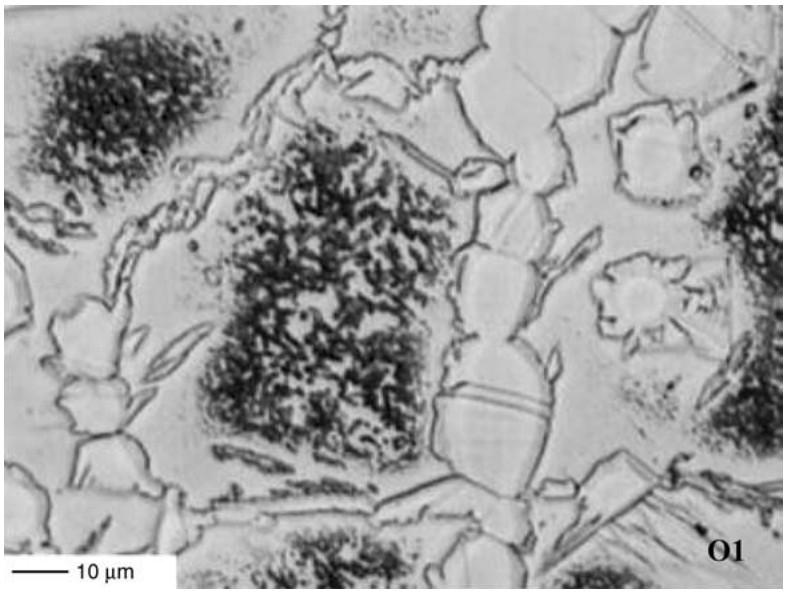

Figure 6 Microstructure of the oil cooled sample (O1) revealed by electrolytic etch in oxalic acid solution.

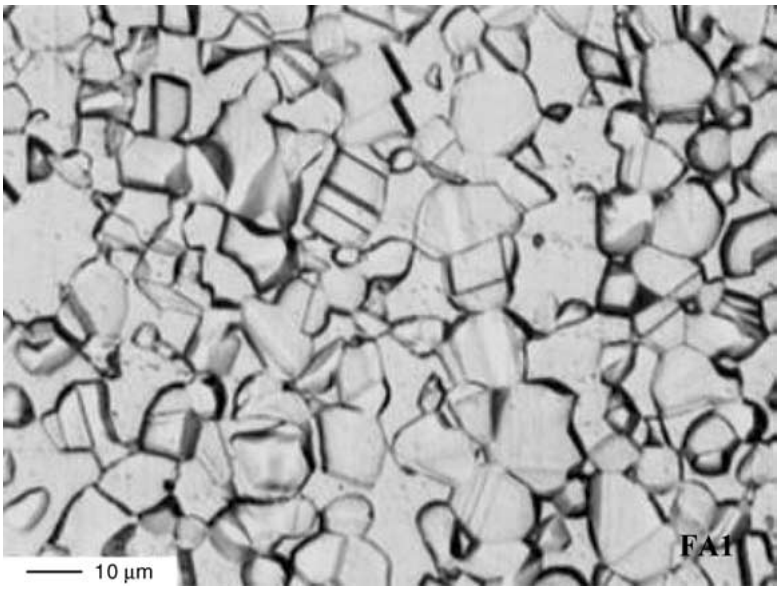

Figure 7 Microstructure of the sample FA1 revealed by electrolytic etch in oxalic acid solution.

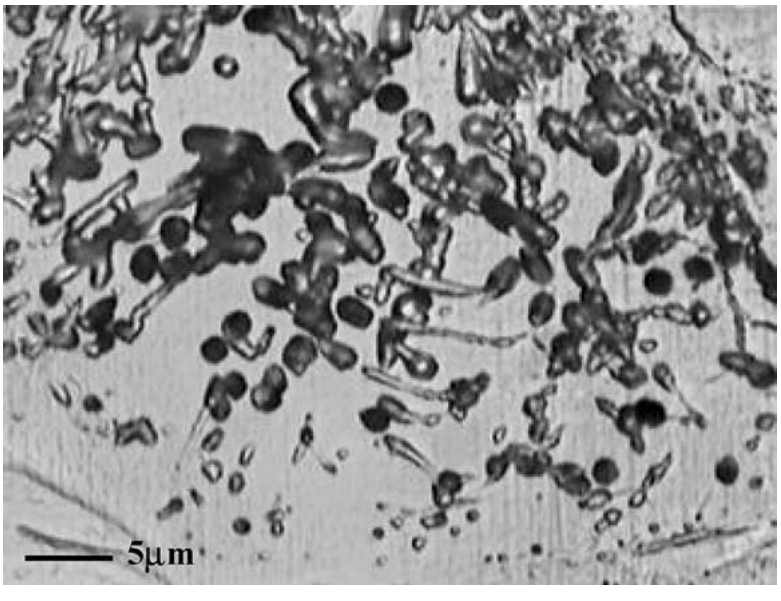

Figure 8 Detail of the chromium nitride precipitation in the ferrite phase of sample O1.

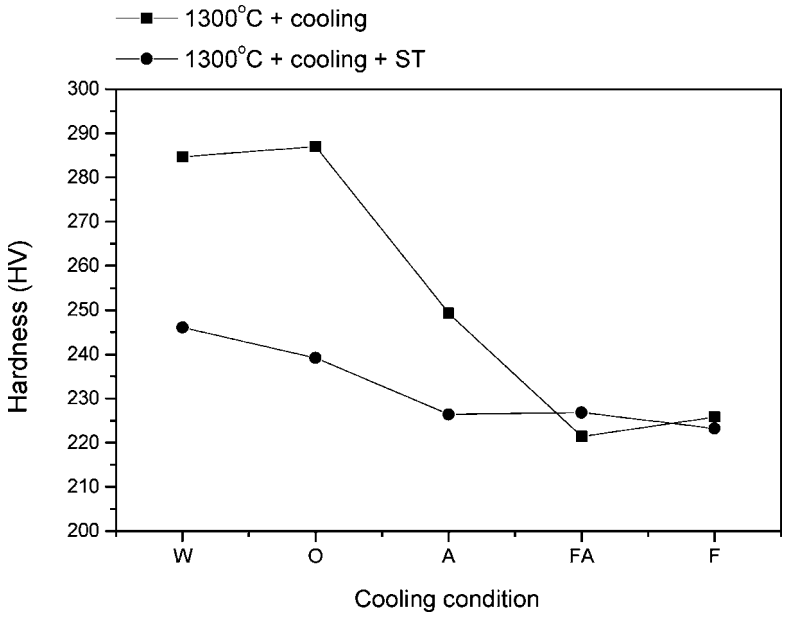

Figure 9 Hardness as function of cooling condition before and after the solution treatment (ST).

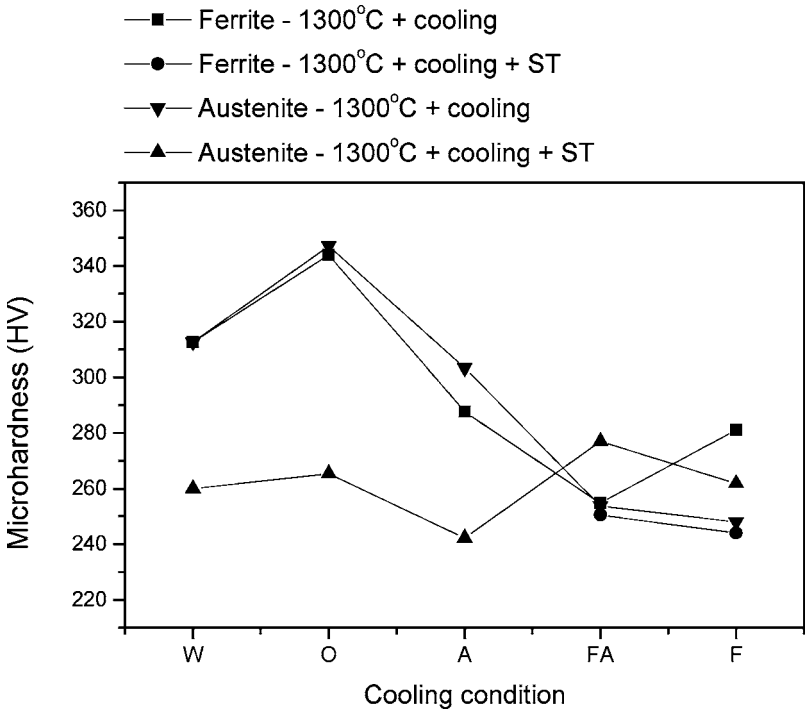

Figure 10 Microhardness of ferrite and austenite as function of cooling condition before and after the solution treatment (ST).

hardness value is attained in the sample FA1, which also presents the higher toughness value. The water and oil cooled samples (W1 and O1) present the higher hardness and lower toughness values. At these conditions the austenite content is very small (17.1 and 27.6%) which favours the nitrogen segregation in the ferrite phase and the precipitation of Cr_2N on cooling. Besides this, the lower austenite fraction also allows a larger ferrite grain size (Figs 5 and 6).

Fig. 10 shows that the microhardness of the ferrite phase is still higher in the sample O1 than in sample W1, probably because the lower cooling rate of sample O1 allows a more intense Cr_2N precipitation. The austenite phase is also very hard in the fast cooled samples, since the few austenite islands dissolve a high nitrogen content, as will be shown later. It is a matter of discussion if the high nitrogen alloyed austenite in the grain boundaries of the fast cooled samples plays an embrittlement hole or not. In our opinion, based in a previous work [6], it does, but is a less important factor when compared to the chromium nitride precipitation and the large ferrite grain size.

The fracture surface of the fast cooled samples (W1 and O1) presented a mixture of brittle and ductile portions (Fig. 11), while the FA1 sample presented a completely ductile fracture (Fig. 12). The solution treated samples also presented a completely ductile fracture (see Fig. 13, as an example).

The solution treatment at 1000°C followed by water cooling promotes an increase of toughness in all conditions and softening in the fast cooled ones (see Figs 4 and 9). The structure of fast cooled samples is completely modified by this treatment: small austenite particles precipitate into the ferrite domains promoting a desirable grain refinement; the austenite volume fraction increases to the equilibrium value (0.55–0.60); the Cr_2N particles are dissolved and the nitrogen is redistributed into the austenite phase.

Fig. 14 shows the X-ray diffractograms of the samples water (W1) and furnace (F1) cooled. The ferrite and austenite peaks of the sample W1 are displaced to the left. The austenite parameter has increased from 3.603 to 3.621 Å and the ferrite parameter has increased from 2.878 to 2.886 Å. This shift is caused by the increase of the nitrogen content in both phases, mainly in the austenite. An estimation of the effect of nitrogen on the austenite parameter (a_γ) can be obtained by fitting the a_γ values of fcc FeN_x solid solutions against the atomic fraction (x) or weight percentage (%wt.N) of nitrogen. It was done using the JCPDS data base [7] for x varying from 0.0324 to 0.095 and it is found that each 1%wt. N causes an unit cell volume variation (ΔV) of about 1.411 $Å^3$. As the ΔV between the austenite of the two samples is $(3.621)^3 - (3.603)^3 = 0.704$ $Å^3$, the austenite of the water cooled sample must contain about 0.50%wt. N more than the furnace cooled one. This explain the higher microhardness value of the water cooled sample (Fig. 10).

The cooling rate of duplex welds must be high enough to obtain at least 35% of austenite and fast enough to avoid sigma phase, chromium carbide and α' precipitation. Sample F1 (furnace cooled from 1300°C to RT) presented the highest austenite content but a low toughness value (29 J). X-ray diffraction analysis (Fig. 14) and scanning electron microscopy observation have not shown any trace of sigma phase in the furnace cooled sample, but some intergranular carbides were revealed by the electrolytic etch (Fig. 15). On the other hand, the increase of microhardness of the ferrite phase from sample FA1 (254 HV) to sample F1 (281 HV) (Fig. 10) is an indication that the initial stage of the spinodal decomposition has occurred in the ferrite phase. This is in agreement with the work of Lemoine *et al.*

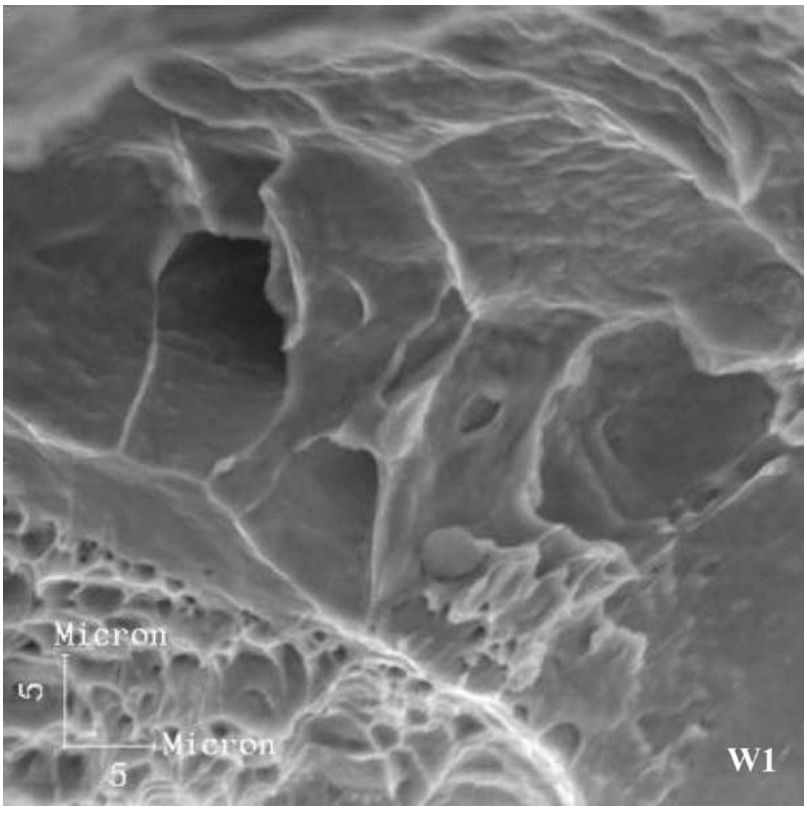

Figure 11 Surface fracture of sample W1 showing brittle (upper) and ductile (down) regions.

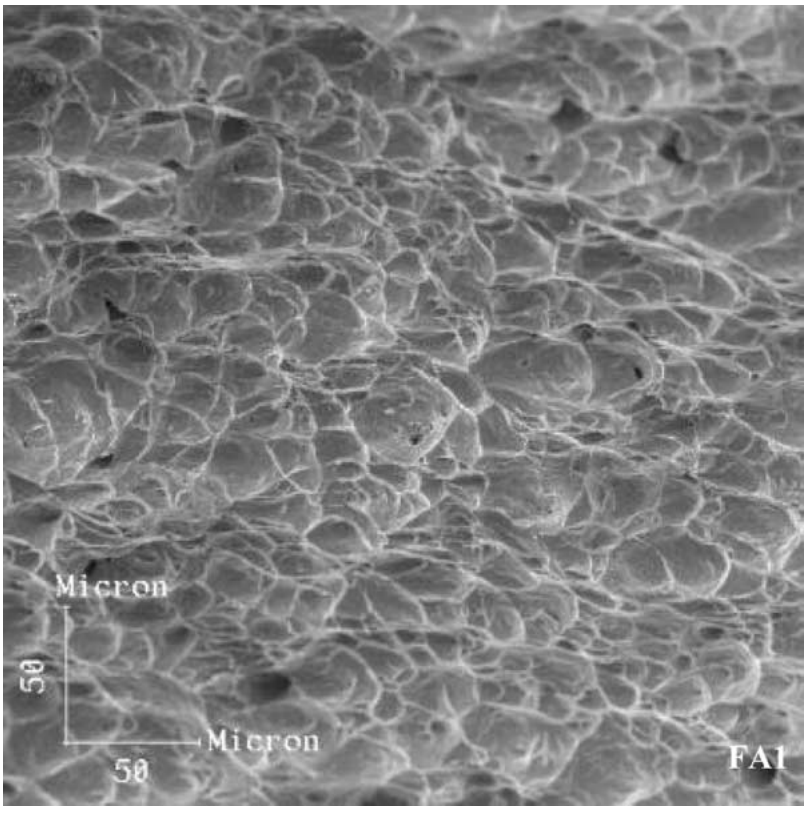

Figure 12 SEM image of the surface fracture of the sample FA1.

[8]. They showed the influence of the cooling rate from 1080°C to room temperature on the ferrite decomposition of a cast DSS and found that the increase of the cooling rate from 2 to 5°C/s caused the increment of the microhardness of ferrite from 304 to 348 HV.

The fractographic examination of the sample F1 (Fig. 16) show the brittle areas and carbide particles. The increase of toughness obtained with the solution treatment in this condition (see Fig. 4), is due to the dissolution of the chromium carbides and the elimination of chromium fluctuations present in the begin of spinodal decomposition. As expected, the microhardness of the ferrite phase decreases with the solution treatment.

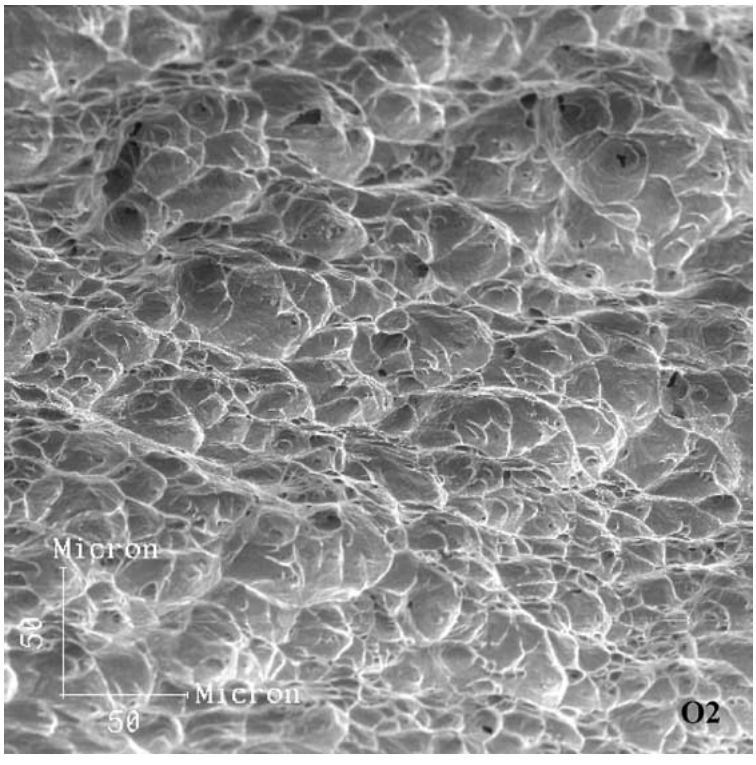

Figure 13 SEM image of the surface fracture of sample O2.

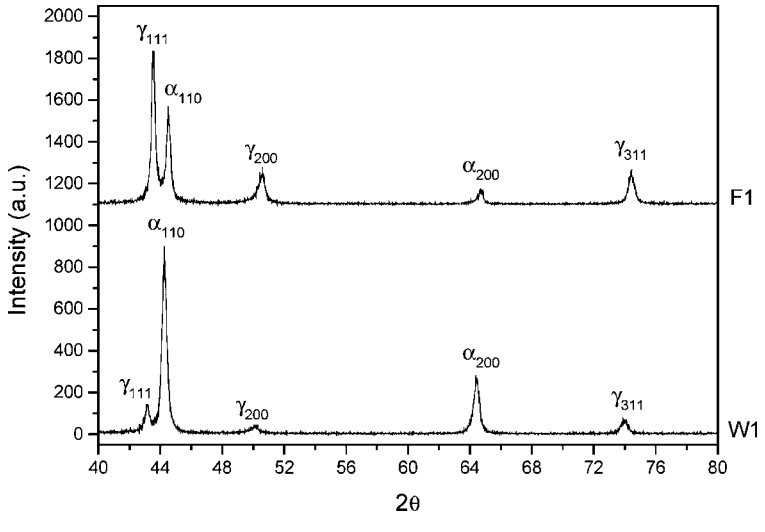

Figure 14 X-ray diffraction of samples F1 and W1.

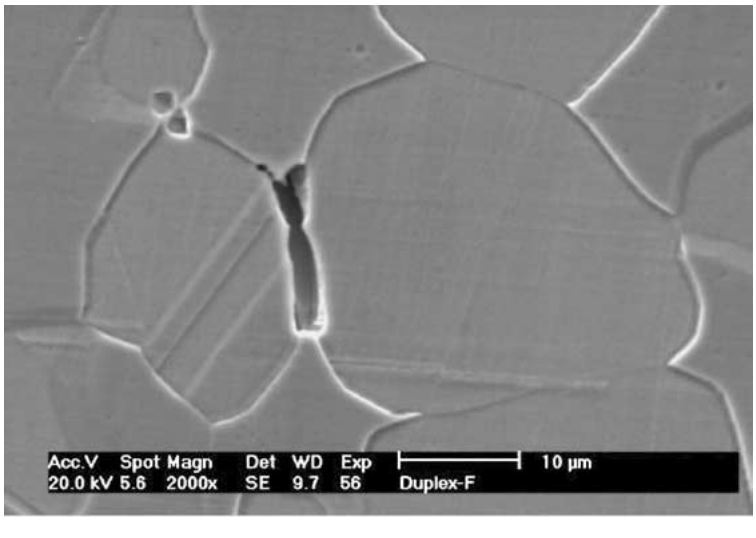

Figure 15 SEM image of the microstructure of the sample F1 revealed by electrolytic etch in oxalic acid solution.

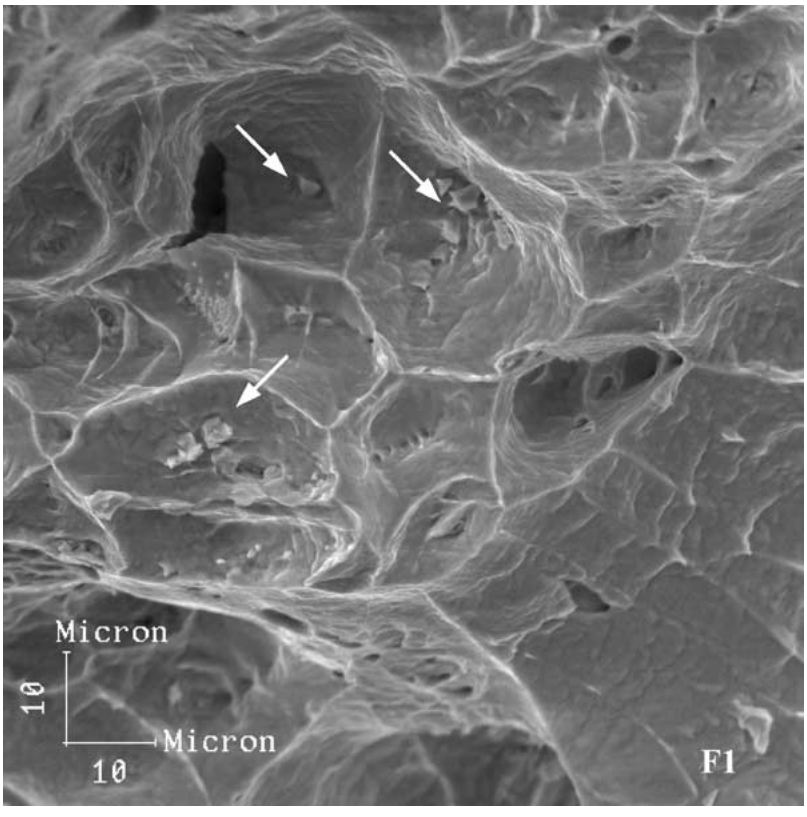

Figure 16 SEM image of the surface fracture of the sample F1.

4. Conclusions

The microstrucutre of the duplex stainless steel investigated in this work presented 17.1 and 27.6% of austenite after water and oil cooling from 1300°C, respectively. Due to such a low austenite content the ferrite grains became very coarse and chromium nitride has precipitated in the ferrite matrix. Consequently the toughness of these samples resulted very low, and surface fracture presented a mixture of ductile and brittle portions even at room temperature tests.

The higher toughness was obtained in the sample furnace cooled from 1300 to 1000°C and air cooled from this to room temperature. At this condition a fine microstructure with 55.4% of austenite was obtained.

However, if the sample is furnace cooled from 1300°C to room temperature, the low cooling rate below 1000°C may promote the undesirable precipitation of chromium carbides. Such a low cooling rate has also increased the microhardness of the ferrite phase, which is an indication of the begin of the spinodal decomposition process in the 550–350°C range. As result the toughness of this sample was low, despite of its high austenite content and fine grain structure.

The solution treatment at 1000°C followed by water cooling promotes an increase of toughness in all conditions. In the fast cooled samples the following changes are observed: small austenite particles precipitate into the ferrite domains promoting a desirable grain refinement; chromium nitride particles are dissolved and the nitrogen redistribution in the austenite phase is allowed, as observed by lattice parameters measurements. The solution treatment also improved the toughness of the furnace cooled sample since it eliminates the intergranular chromium carbides and reverts the spinodal decomposition of the ferrite phase.

Acknowledgements

The authors would like to acknowledge the Braziliam research agencies CNPq and FAPERJ for financial support.

References

1. ASM Speciality Handbook, "Stainless Steels," 1994.
2. J. D. KORDATOS, G. FOURLARIS and G. PAPADIMITRIOU, *Mater. Science Forum* **318–320** (1999) 615.
3. J. D. KORDATOS, G. FOURLARIS and G. PAPADIMITRIOU, *Scripta Mater.* **44** (2001) 401.
4. P. KRULL, H. PRIES, H. WOHLFAHRT and J. TÖSCH, *Welding and Cuttung* **11** (1997) 2.
5. Annual Book of ASTM Standarts, Designation E-23-94b, p. 137, 1995.
6. S. S. M. TAVARES, J. M. NETO and M. R. DA SILVA, *J. Alloys Comp.* **313** (2000) 168.
7. JCPDS Data Base of X-ray Diffraction (CD-ROM), International Centre of Diffraction Data, 2000.
8. C. LEMOINE, A. FNIDIKI, F. DANOIX, M. HÉDIN and J. TEILLET, *J. Phys.: Condens. Matter* **11** (1999) 1105.

Received 26 September 2003
and accepted 12 August 2004